

Dark Matter perspective of Left-Right symmetric gauge model

Sanchari Bhattacharyya* and Anindya Datta†

*Department of Physics, University of Calcutta
92, Acharya Prafulla Chandra Road, Kolkata 700009*

Abstract

We consider an incarnation of left-right symmetric model with a local gauge symmetry of $SU(3)_C \otimes SU(2)_L \otimes U(1)_L \otimes SU(2)_R \otimes U(1)_R$. Heavy scalars and fermions present in the **27** of E_6 are included in the matter sector along with the Standard Model fermions. Two such colour singlet fermions, N and l_S , transforming as bi-doublet and singlet under $SU(2)$ s respectively, can be potential candidates for Dark Matter (DM). Assignment of $U(1)$ charges for the matter fields restricts some of the exotic fermions to interact with the SM fermions. We study in some details the prospect of such fermionic dark matters by calculating relic densities and direct detection cross-sections by treating these particles as stand alone relic particles in turn. N , when treated as relic particle, would produce a direct-detection cross-section very high compared to the experimental upper limits. However, the interaction rate of N can be controlled by introducing a dimension-6 operator involving two N fields and two SM fermions and appropriately choosing the coupling constant. This in turn, makes the interaction rate of N very high and yields a small relic density. On the other hand, l_S for some chosen mass window, can give us right amount of relic, but its direct detection cross-section is too small. Keeping these in mind, we propose two-component model of DM, where both N and l_S contribute to the relic density, albeit with unequal proportion. While, the direct detection cross-section limits can be satisfied mainly by N in presence of an extra dimension 6 interaction. We derive limits on such an interaction from XENON experiment.

1 Introduction

In recent times, several cosmological parameters have been measured experimentally at unprecedented precision. One such example is the experimental data from several independent experiments, mounting to unavoidable evidence in support of a non-luminous matter, more commonly known as Dark Matter (DM) present in the entire Universe. The measurement from the PLANCK [1] reveals that luminous matter constitutes only 4-6% of the energy density of the Universe whereas almost 26% of it is accounted by DM, whose exact nature is still an enigma to us. This partitioning of energy density of the Universe has also been in agreement with the measurement of CMBR anisotropy from WMAP [2]. Indirect evidences in support of existence of DM have also been gathered more recently, from satellite based experiments like AMS [3], PAMELA [4] and Fermi-LAT [5,6].

On the particle physics front, discovery of the Higgs boson [7] and the ongoing measurement of its properties at the Large Hadron Collider (LHC) experiment once again has firmly established the validity of the Standard Model (SM) at TeV scale. However, the absence of a viable DM candidate and massive neutrinos are major shortfalls of the so far successful model of interactions among elementary particles and fundamental forces. Although, in earlier times, weakly interacting neutrinos have been thought to be the candidates for the DM, with advent of more and more precise cosmological data, neutrinos are disfavoured.

*sanchari1192@gmail.com

†adphys@caluniv.ac.in

The demand for a viable DM candidate has been one of the main motivations to look beyond the SM (BSM). In the post Higgs-boson discovery era, pursuit for a dark matter is the prime aim for experimental and theoretical front. Supersymmetric (SUSY) [8, 9] and extra-dimensional models [10] have been so far very popular and thus extensively investigated scenarios beyond the SM. Imposition of a Z_2 -symmetry (R -parity for SUSY and KK -parity for extra-dimensional models) on the action, ensures the stability of the lightest SUSY (KK) particle which can be a viable DM candidate. However, non-observation of any tele-tale signature of any kind of new physics from the LHC, only has pushed the lower mass limits of SUSY or KK -particles in the TeV range [11]. Several other variants of DM models have also been proposed. Little Higgs model [12], models with extended scalar sector [13] or an $U(1)$ extended SM [14] are notable among them. One common feature of all such BSM extensions is that, the stability or weakness of the DM candidate(s) in such models are ensured by demanding an ad-hoc discrete symmetry (generally a Z_2) of the action. This symmetry have different incarnations in different BSM scenarios, like R -parity in SUSY, KK -parity in extra-dimensional models or T -parity in Little Higgs model.

In the present article, we will turn our attention to an unifying gauge group E_6 [15], which can be broken down to $[SU(3)]^3$ followed by a further breakdown to $SU(3)_C \otimes SU(2)_L \otimes U(1)_L \otimes SU(2)_R \otimes U(1)_R$ (32121). The main advantage of working in a framework of unifying group like E_6 is the natural appearance of right-handed neutrinos as well as 3 generations of heavy neutral leptons, singlet under either of $SU(2)$ groups. Assignments of hyper-charges (for these fermions, from the consideration of anomaly cancellation) restrict SM fermions to have couplings with the exotic fermions and some of the Higgs bosons. This in turn pave the way for some of the fermions (with zero electric charge) to be viable DM candidates. A more detailed discussion about this model and its phenomenology in the context of the LHC has been discussed in a previous article [16]. In this article, we will concentrate on the viable candidates of DM in 32121 model, whether the masses and interactions of such particles are in the right ball park to satisfy the relic density and direct detection limits obtained from experiments.

Fermionic dark matter is not a very novel concept. Previously many authors [14, 17, 18] have studied the possibility of a DM which has spin $\frac{1}{2}$, both Dirac and Majorana in nature with their masses varying from sub-MeV scale to TeV scale. However in all of these studies, the SM has been augmented by such fermionic fields, which couple to the SM via either a scalar or a gauge boson not present in the SM. Moreover, couplings of such exotic particles to the SM have been restricted by imposing some extra discrete symmetry on the action or in some cases such an extra symmetry is a remnant of breakdown of some bigger symmetry already existing in the action [18]. However, in most of these studies, the spin $\frac{1}{2}$ DM, is accompanied by another relic particle also having restricted coupling to SM particles. The scalar relic also contributes to Ωh^2 and takes part in direct detection process. However, novelty of our analysis lies in the presence of a pair of spin $\frac{1}{2}$ relic particles, one Dirac and the other Majorana in nature along with few other fermions, arising from the full **27**-plet of E_6 . We have already mentioned that we need not to impose any discrete symmetry to restrict the couplings of the DM candidates to the SM fields. Such couplings have been automatically not allowed from the $U(1)_{L,R}$ assignments of such fermions. It is important to mention that few of these exotic fermions (which have electromagnetic/weak charges) also play a crucial role in co-annihilation processes thus indirectly contribute to relic density. This is certainly a hallmark of a more *complete* BSM like MSSM, where the extra particle fields arise to fulfill the conditions of full symmetry of the theory. Furthermore, in our case, gauge symmetry allows a Higgs mediated interaction between two DM candidates, which we will see, plays a crucial role in determining the relic density.

In the next section (Section 2), we will briefly review the 32121 model with emphasis on the possible DM candidates and their interactions. Section 3 will deal with the issue of direct detection of the DM on earth bound experiments. We will estimate the DM nucleon cross-section and compare the results with experimental data from XENON, LUX and PICO. We shall also discuss a very brief outline of the standard route to relic abundance calculation starting from the interactions and identification of annihilation and co-annihilation channels relevant for the estimation of relic density. In section 4, we shall investigate the two-component dark matter scenario and present the main results of our analysis in this case. Finally we conclude in section 5.

2 Description of 32121 Model

We are interested in a left-right (LR) symmetric gauge group $SU(3)_C \otimes SU(2)_L \otimes U(1)_L \otimes SU(2)_R \otimes U(1)_R$. This can be a result of two step breaking of E_6 . We are not interested in the exact mechanism of this breaking chain, at this moment. As we need some new particles apart from the SM fermions or scalars, the particle content of SM has been augmented by more than one fermions present in **27**-plet of E_6 . This choice of fermions, with charge assignments listed in Table 1. The assignment of all the gauge quantum numbers is anomaly free.

Gauge bosons present in this model automatically follow from the gauge group. The matter and gauge fields

which are present in our model including the Higgs multiplets along with the gauge quantum numbers instrumental in breaking down $SU(3)_C \otimes SU(2)_L \otimes U(1)_L \otimes SU(2)_R \otimes U(1)_R$ to the SM gauge group are listed in Table 1. Electric charge, Q is defined through the relation, $Q = T_{3L} + T_{3R} + Y_L/2 + Y_R/2$. L and R stand for left and right respectively.

| | | 3_C | 2_L | 2_R | 1_L | 1_R |
|--------------|------------------------|-----------|-------|-------|-------|-------|
| Fermions | \bar{L}_L | 1 | 2 | 1 | -1/6 | -1/3 |
| | \bar{L}_R | 1 | 1 | 2 | 1/3 | 1/6 |
| | \bar{L}_B | 1 | 2 | 2 | -1/6 | 1/6 |
| | \bar{L}_S | 1 | 1 | 1 | 1/3 | -1/3 |
| | Q_L | 3 | 2 | 1 | 1/6 | 0 |
| | \bar{Q}_R | $\bar{3}$ | 1 | 2 | 0 | -1/6 |
| | \bar{Q}_{LS} | $\bar{3}$ | 1 | 1 | -1/3 | 0 |
| | Q_{RS} | 3 | 1 | 1 | 0 | 1/3 |
| Higgs Bosons | Φ_B | 1 | 2 | 2 | 1/6 | -1/6 |
| | Φ_L | 1 | 2 | 1 | 1/6 | 1/3 |
| | Φ_R | 1 | 1 | 2 | -1/3 | -1/6 |
| | Φ_S | 1 | 1 | 1 | -1/3 | 1/3 |
| Gauge bosons | $G^i, i = 1, \dots, 8$ | 8 | 1 | 1 | 0 | 0 |
| | $W_L^i, i = 1, 2, 3$ | 1 | 3 | 1 | 0 | 0 |
| | $W_R^i, i = 1, 2, 3$ | 1 | 1 | 3 | 0 | 0 |
| | B_L | 1 | 1 | 1 | 0 | 0 |
| | B_R | 1 | 1 | 1 | 0 | 0 |

Table 1: Fermions and Bosons in 32121 model with their respective quantum numbers

2.1 Description of the Scalar, Gauge and Fermion sector

Scalar sector: The scalar sector of the 32121 model contains one Higgs bi-doublet (Φ_B), one left-handed (Φ_L), one right-handed (Φ_R) weak doublets and a singlet Higgs boson (Φ_S) with non-zero $U(1)_{L,R}$ charges. These scalars arise from the $(\mathbf{1}, \mathbf{3}, \mathbf{\bar{3}})$ representation of $[SU(3)]^3$. For a complete symmetry breaking mechanism from $32121 \rightarrow SU(3)_C \otimes SU(2)_L \otimes U(1)_Y \rightarrow SU(3)_C \otimes U(1)_{EM}$, one needs a bi-doublet scalar field Φ_B , two doublets Φ_L and Φ_R along with a $SU(2)$ singlet Higgs field Φ_S . Five neutral CP-even scalars ($h^0, h_2^0, h_L^0, H_R^0, H_S^0$), two CP-odd scalars (ξ_2^0, ξ_L^0) and two charged scalars (H_1^\pm, H_L^\pm) are left after EWSB. One from the CP-even sector (h^0) is identified with the SM Higgs boson. Two neutral scalars, h_L^0 and ξ_L^0 (originating from Φ_L) having minimal interaction to other SM particles could be possible relic particles and we will see whether they could satisfy the limits of relic density and scattering cross-section from direct detection of DM.

Gauge sector: The electro-weak gauge sector of 32121 model consists of two charged gauge bosons W, W' and four neutral gauge bosons. Two of them can be identified with the SM-like Z boson and photon. The remaining two massive neutral gauge fields are identified as Z' and A' where the appearance of A' is the consequence of the extra local $U(1)$ symmetry. Their masses and interactions are governed by 4 gauge coupling constants g_{2L}, g_{2R}, g_{1L} and g_{1R} and non-zero vacuum expectation values (vevs) of the scalar fields. However, in order to keep our Lagrangian manifestly LR symmetric, we assume $g_{2L} = g_{2R}$ and $g_{1L} = g_{1R}$. All our analysis presented in the following will be based on this assumption. The vevs of the scalar fields can be constrained from below from the experimental lower limit of heavy gauge boson masses. For a detailed discussion about the gauge sector we refer the reader to an earlier work [16].

Fermion sector: Apart from SM fermions, the model under consideration contains a right-handed neutrino ν_R , an $SU(2)_L \times SU(2)_R$ singlet quark q_S , (a Dirac fermion constructed out of Weyl fermions Q_{LS} and Q_{RS}) and E (N) transforming non-trivially under $SU(2)_L \times SU(2)_R$ (a Dirac fermion constructed out of Weyl fermions E_1 (N_1) and E_2 (N_2)). The gauge quantum numbers of the fermions used in our analysis have been listed in Table 1. Apart from these, we also have a $SU(2)$ singlet charge neutral lepton l_S in the spectra. Both N and l_S can be viable dark matter particles.

Fermions get their masses via the interactions with Higgs fields. The relevant Yukawa Lagrangian is noted below.

$$\begin{aligned}\mathcal{L}_{Yukawa} = & y_{qij} \bar{Q}_{iL} \Phi_B Q_{jR} + \tilde{y}_{qij} \bar{Q}_{iR} \tilde{\Phi}_B Q_{jL} + y_{lij} \bar{L}_{iL} \Phi_B L_{jR} + \tilde{y}_{lij} \bar{L}_{iR} \tilde{\Phi}_B L_{jL} \\ & + y_{sij} \bar{Q}_{iLS} \Phi_S Q_{jRS} + y_{LBij} \text{Tr} \left[\bar{L}_{iB} \tilde{L}_{jB} \right] \Phi_S^c + \frac{y_{LSij}}{\Lambda} \bar{L}_{iS} L_{jS}^c \Phi_S \Phi_S \\ & + y_{BBij} \text{Tr} \left[\bar{L}_{iB} \tilde{\Phi}_B \right] L_{jS}^c + H.C.\end{aligned}\quad (1)$$

where, $i, j = 1, 2, 3$ are generation numbers and $y(s)$ are Yukawa coupling constants. Φ_S^c is complex conjugate of Φ_S , $\tilde{\Phi}_B = \sigma_2 \Phi_B^* \sigma_2$, $\tilde{L}_B = \sigma_2 L_B^* \sigma_2$.

Yukawa interactions which in turn generate masses for the SM fermions are noted in the first line of Eq. 1. It is interesting to note, one can only write Yukawa interactions of the SM fermions to the bi-doublet Higgs Φ_B while exotic fermions can get their masses via their interactions with the singlet Higgs field Φ_S (see the second line of Eq. 1) only. This is a consequence of assignments of $U(1)_{L,R}$ charges of the fermions and scalars. A notable advantage of absence of such interactions between exotic and SM fermions facilitate us to choose N and/or l_S to be a DM candidate. One does not have to impose any discrete symmetry on the fields to prevent the DM particle from decaying to a pair of lighter SM particles. One may connect this to the breaking of E_6 down to 32121 [19].

The Yukawa coupling matrices, y_q, y_l, y_{LB}, y_s are considered as non-diagonal. It is important to mention that there are no such term present in the Yukawa Lagrangian that leads to mixing among exotic and SM fermions. So the mass matrices of SM and exotic fermions can be brought into diagonal form independent of each other. Thus while considering the phenomenology of some of the exotic fermions, we may use their physical masses as the free parameters of the analysis.

It is important to note, a dimension-4 mass term for the singlet lepton l_S (a Weyl spinor) cannot be written as it transforms non-trivially under $U(1)_{L,R}$. But we are able write a dimension-5 operator, which in turn generates mass for l_S . To generate a mass using Higgs mechanism, one must employ a fermion from a multiplet of E_6 other than **27** (e.g., **78** representation). So Λ may be identified with the mass of such a fermion.

The last term in Eq. 1 seeks our attention. It introduces a mixing between the singlet lepton (l_S) and the charge neutral lepton (N) via the bi-doublet Higgs boson Φ_B . The mass term in the Yukawa Lagrangian can be written in (N_1, N_2, l_S^c) basis is as follows.

$$(\bar{N}_1 \quad \bar{N}_2 \quad \bar{L}_S) \begin{pmatrix} 0 & \sqrt{2} y_{LB} v_S & 0 \\ \sqrt{2} y_{LB} v_S & 0 & 0 \\ 0 & \frac{y_{BB}}{\sqrt{2}} k_1 & \frac{y_{LS}}{2\Lambda} v_S^2 \end{pmatrix} \begin{pmatrix} N_1 \\ N_2 \\ L_S^c \end{pmatrix} \quad (2)$$

Given the fact that $k_1 \ll v_S$, the terms proportional to y_{BB} will introduce a nominal mixing between N and l_S . For all practical purpose, N and l_S are the physical eigenstates. The corresponding eigenvalues will be used as free parameters in our analysis without any loss of generality. However, we will see that this particular interaction will play a crucial role while evaluating the relic density in case of a two-component DM scenario comprising of N and l_S .

This mixing will also generate a mass difference between E and N but the mass splitting will be very small ($\mathcal{O}(y_{BB}^2 k_1^2 / m_N)$) compared to m_E or m_N . In this study, it is necessary for E to be heavier than N so that it can decay and thus does not contribute to the relic. The necessary mass difference between N and E could be thought to be generated via some other interactions like electro-weak/magnetism.

2.2 Dark Matter Candidates in 32121

With a careful study of the particle sector of 32121 model, one can identify a number of new particles who could be eligible candidates for the dark matter. A suitable DM candidate must,

- be stable (or for decaying DM, lifetime $>$ age of the Universe) and possibly charge neutral.

- satisfy the limits on relic abundance of the Universe in present epoch.
- agree with the upper limits on DM-nucleon scattering cross-section obtained from the direct detection experiments.
- agree with the limits on decay branching ratio [20] of SM-Higgs to invisibles.

In the following we discuss quantitatively the prospects of some of the suitable DM candidates in this model.

h_L^0 and ξ_L^0 are degenerate in mass. Due to their mass degeneracy direct detection cross-section of such scalar dark matter is well above the limit coming from an experiment like XENON [21]. By the same token of argument their annihilation cross-section to the SM particles is very high resulting into a very tiny relic density well below the PLANCK limit. We abandon the case of scalar dark matters and focus into fermionic dark matter in our following analysis.

DM candidates arising from fermion sector: Eq. 1 reveals that the mixing of exotic fermions with SM fermions are prohibited and exotic fermions cannot decay to a pair of SM particles. In such a scenario, the two neutral exotic leptons N and l_S can be eligible DM candidates.

Now, in the other scenario when the last term in Eq. 1 is switched on, some new interactions come into play which may make any one of l_S or N to be unstable. For example, turning on y_{BB} gives rise to some interactions among N , l_S , E^\pm and the neutral (h^0 , ξ_2^0 , h_2^0 , H_S^0) and charged scalar (H_1^\pm). In such a case, the mass difference between N and l_S plays an important role in co-annihilation of the DM. However, in a single DM scenario, the lightest between N and l_S will be the relic particle. In the next section, we will first consider the direct detection mechanism of N or l_S treating each of them to be the DM candidate followed by an estimation of relic abundance.

3 Study on the Dark Matter in 32121 Model

In the previous section, we have identified the particles which can satisfy the DM criteria. In this section, we shall mainly concentrate on the detail analysis of the aforementioned WIMP-like DM candidates. We have investigated the DM-nucleon scattering cross-sections and compared the results with the experimental data by XENON collaboration [22] and other experiments like LUX [23] and PICO [24]. Next, we will analyse whether they can satisfy present DM relic abundance of the Universe [1].

3.1 Direct Detection of Dark Matter

First we concentrate on the elastic scattering between the nucleus and dark matter candidate. Experiments like XENON [22], LUX [23], PANDA [25] provide upper limits on the DM-nucleon scattering cross-section. We have considered two fermionic dark matter candidates, namely N , a Dirac fermion and l_S which is a Majorana-like fermion.

For a generic fermionic DM, χ (which can be identified with N or l_S in our model), the quark-level effective operators, responsible for its direct detection are the following,

$$\mathcal{C}_s (\bar{\chi}(g_{\chi s} + ig_{\chi p}\gamma^5)\chi) (\bar{Q}(g_s + ig_p\gamma^5)Q) \quad (3)$$

$$\mathcal{C}_v (\bar{\chi}\gamma^\mu(g_{\chi V} + g_{\chi A}\gamma^5)\chi) (\bar{Q}\gamma_\mu(g_V + g_A\gamma^5)Q) \quad (4)$$

Here, Q is a SM-quark field. Eq. 3 represents the case where a scalar particle acts as a mediator. $g_{\chi s(p)}$ is the coupling between DM and mediating scalar (pseudo-scalar) while $g_{s(p)}$ are couplings between the mediator scalar (pseudo-scalar) with a pair of SM-quarks. Similar definition holds for the couplings in Eq. 4 too except the fact that here the mediator is one of the heavy neutral gauge bosons of 32121 model. $V(A)$ stands for vector (axial vector) mediation in such a case. $\mathcal{C}_{s,v}^{-1}$ is connected to the square of the mass of the scalar or vector mediator (see Fig. 1).

Fig. 1 shows the tree-level Feynman diagrams which will lead to the aforementioned effective operators in Eqs. 3, 4. Following Eq. 1, considering the parameter space mentioned in [16] (where mixing between H_R^0 and h^0/H_S^0 is almost vanishing) it is clear that the mediating scalar could be either h^0 or H_S^0 .

The Higgs mediated diagram in Fig. 1 will be suppressed with respect to the gauge mediated diagram due to the following reasons. Primarily Higgs couplings to the SM quarks are proportional to the quark masses thus are

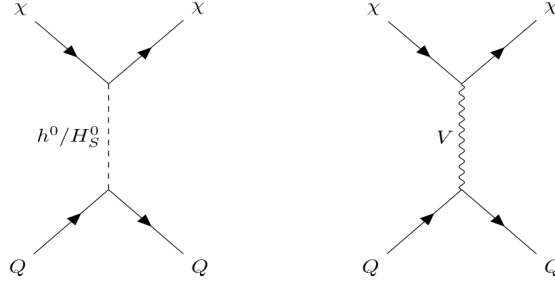


Figure 1: The tree-level Feynman diagrams corresponding to the operators in Eq. 3 (left) and Eq. 4 (right). V represents a massive neutral gauge boson of 32121 model.

small. Secondly, the dark matter (N or l_S) scatters off the quarks via its interaction to H_S^0 whose admixture in the relevant Higgs eigenstate is very small [16]. Spin-dependent DM-nucleon cross section which follows from Eq. 3 will be further suppressed by the powers of DM speed. Consequently contributions from such diagrams to total detection the cross-sections will be negligible.

Eq. 4 points towards spin-1 vector boson mediated DM-quark scattering corresponding to the right diagram in Fig. 1. It results into both spin-independent and spin-dependent cross-sections depending on the vector and axial vector-like couplings the associated particles have. The vector mediated spin-independent cross-section will be,

$$(\sigma_{SI})_V \simeq \frac{g_{\chi V}^2 \mu_{\chi N}^2}{\pi m_V^4} \left[\tilde{f}_p Z + \tilde{f}_n (A - Z) \right]^2 \quad (5)$$

\tilde{f}_p and \tilde{f}_n are dimensionless quantities, involving the couplings of the quarks with the mediating gauge bosons, $\mu_{\chi N}$ is the reduced mass of the WIMP-nucleus system [26].

The spin-dependent cross-section can also be expressed as the following,

$$(\sigma_{SD})_V \simeq \frac{4g_{\chi A}^2 \mu_{\chi N}^2}{\pi m_V^4} J_N (J_N + 1) \left[\frac{\langle S_p \rangle}{J_N} \tilde{a}_p + \frac{\langle S_n \rangle}{J_N} \tilde{a}_n \right]^2 \quad (6)$$

$\tilde{a}_{p,n}$ are dimensionless quantities, J_N is the spin of the nucleus, $\langle S_{p,n} \rangle$ are the average spin of the nucleons [26].

For 1 TeV mass of N , $\sigma_{SI} = 4.466 \times 10^{-13}$ pb and $\sigma_{SD} = 4.08 \times 10^{-2}$ pb for proton-DM (N in this case) scattering. We have observed that σ_{SD} is order of magnitudes higher than σ_{SI} and it also exceeds the upper limit of DM-nucleon scattering cross-section from PICO [24]. In order to rescue N from such a conflict with experimental result, a dimension-6 four-fermion operator has been introduced (see Eq. 7), with a hope that an appropriate choice of the effective coupling (ϵ'/Λ'^2) could bring this spin-dependent cross section within the experimental limit.

$$\frac{\epsilon'}{\Lambda'^2} \text{Tr}[(\bar{L}_B \gamma^\mu \tau_a L_B)] (\bar{f}_L \gamma_\mu \tau_a f_L + L \leftrightarrow R) \quad (7)$$

Such an interaction could have originated from the scattering of a pair N off the quarks mediated by heavy gauge boson belonging to **78** representation of E_6 . Here, Λ' is a heavy mass scale probably related to the mass of the gauge boson in consideration and $\sqrt{\epsilon'}$ is proportional to the relevant gauge coupling. τ_a s are the Pauli matrices ($a = 1, 2, 3$), f is any SM fermion multiplet. One can see, while calculating the scattering rate, choice of a negative ϵ' can in turn reduce the whole spin-dependent scattering cross-section and satisfy the upper limit on σ_{SD} arising from the present direct detection experiments.

In the following work, we have implemented this model in **FeynRules** [27] and have used the package **micrOMEGAs5.2** [28] to calculate the direct detection cross sections and relic abundances. In Fig. 2, the variation of σ_{SD} for DM-nucleon scattering with ϵ'/Λ'^2 has been shown for three values of masses of N . One can see from Fig. 2, the allowed range of ϵ'/Λ'^2 is $7.43 - 9.06 \times 10^{-6}$ GeV $^{-2}$ ($7.7 - 8.79 \times 10^{-6}$ GeV $^{-2}$) for DM-proton (neutron) scattering. for an N with mass of 1 TeV. The greater the mass of N , a wider range of ϵ'/Λ'^2 is allowed by the data from the experiments like XENON [22], LUX [23] or PICO-60 [24]. The range of values for ϵ'/Λ'^2 allowed from WIMP-neutron scattering are more stringent than the range of values obtained from WIMP-proton scattering (see Fig. 2).

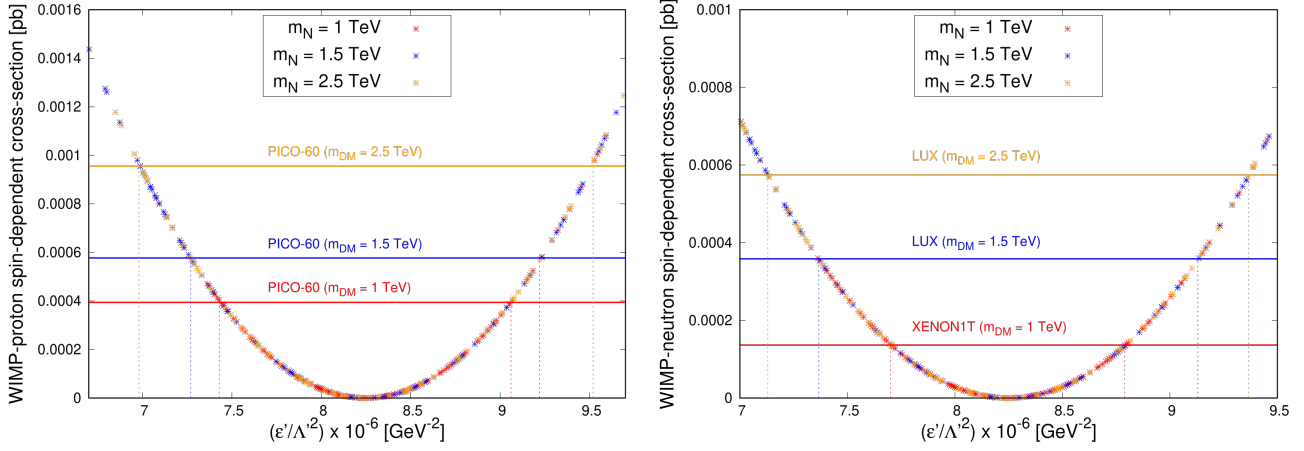


Figure 2: Variation of σ_{SD} with ϵ'/Λ^2 for WIMP-proton (left panel) and WIMP-neutron (right panel) elastic scattering. The red, blue and orange colors correspond to $m_N = 1, 1.5$ and 2.5 TeV respectively. The solid lines represent the upper limits on σ_{SD} from several direct detection experiments.

When l_S is the lightest of all the particles, it can possibly be a candidate for the dark matter. Table 1 shows l_S has exactly equal and opposite $U(1)_{L,R}$ charges which in turn prohibits its coupling to the SM Z -boson however it has axial-vector couplings to heavy gauge bosons A' and Z' . It also couples to scalars via a dimension-5 operator mentioned in Eq. 1. Elastic scattering of l_S with the nucleons are mediated either by scalars or by heavy gauge bosons (see Fig. 1) and can be parametrized via the operators similar to those in Eqs. 3, 4. These interactions are very similar to N apart from the absence of vector like coupling, $g_{\chi V}$ (see Eq. 4) due to the Majorana nature of l_S and contains an extra factor of $\frac{1}{2}$ in each case. The definition of the couplings (g and \mathcal{C}) are similar as in cases of Eqs. 3 and 4.

In all practical purpose, scalar mediated diagrams do not contribute to the elastic scattering cross-section for the reasons mentioned before. Primarily, scalar couplings to the SM quarks are proportional to fermions masses while the scalar coupling to the a pair of l_S is proportional to $\frac{v_s}{\Lambda}$ which could be a number order of one. However, overall rate of this scattering is small due to the small admixture of ϕ_S in the SM Higgs boson [16]. Thus one is left with the contributions from vector mediated processes following Eq. 4 with $g_{\chi V} = 0$ to obtain spin-dependent scattering cross-section of DM over nucleons. We shall have a similar expression like Eq. 6 as σ_{SD} .

Although the rate of gauge mediated process is proportional to gauge couplings, in presence of heavy A' and Z' as the mediator, finally it results into a small σ_{SD} for l_S ($\sim 10^{-10}$ pb over a wide range l_S mass varying from 1 to 4 TeV), well below the experimental upper limits by LUX or PICO.

3.2 Relic Density

In the early Universe, when the temperature of the Universe $T \gg m_\chi$, χ (the particle we consider as dark matter) was abundant and in thermal equilibrium with the SM particles. As the Universe cools down and $T < m_\chi$, χ decouples from the thermal bath. When the annihilation rate of χ is equal to the Hubble expansion rate, it freezes out and the abundance of χ becomes constant. The evolution (with time/temperature) of the number density of the relic particle of our interest can be estimated by Boltzmann equation [29],

$$\frac{dn_\chi}{dt} = -3Hn_\chi - \langle\sigma v\rangle(n_\chi^2 - n_\chi^{eq2}) \quad (8)$$

where, n_χ (n_χ^{eq}) denotes the number density of χ at time t (when in equilibrium), H is Hubble expansion rate and $\langle\sigma v\rangle$ represents the thermally averaged annihilation cross-section of χ times v with v as relative velocity between two DM particles.

N or l_S in general can annihilate to a pair of SM fermions, gauge bosons (neutral and charged) and scalars. For example, annihilation of χ to a pair of SM fermions via gauge bosons can be driven via following interactions.

$$\mathcal{L} \subset m_V^2 V^\mu V_\mu + \bar{\chi}(i\gamma_\mu \partial^\mu - m_\chi)\chi + \bar{f}(i\gamma_\mu \partial^\mu - m_f)f + \bar{f}(g_V \gamma_\mu + g_A \gamma_\mu \gamma^5)fV^\mu + n\bar{\chi}(g_{\chi V} \gamma_\mu + g_{\chi A} \gamma_\mu \gamma^5)\chi V^\mu \quad (9)$$

where g_V ($g_{\chi V}$) and g_A ($g_{\chi A}$) are vector and axial-vector like couplings between SM-fermions (DM candidate χ) and mediating gauge boson respectively. These couplings are solely model-dependent. It is to be noted that $n = 1$ for N (Dirac fermion) and $1/2$ for l_S (Majorana fermion). Further for l_S , $g_{\chi V} = 0$. m_f, m_χ, m_V are the masses for final state fermions, dark matter and mediator respectively.

The thermally averaged cross-section, $\langle\sigma v\rangle$ can be expanded in powers of v^2 or $x(=T/m_\chi)$ (as $v \sim \sqrt{T}$) like,

$$\langle\sigma v\rangle = a_0 + b_0 x + c_0 x^2 + \dots \quad (10)$$

a_0, b_0, c_0, \dots are model dependent constant parameters depending on the couplings and masses of the particles taking part in the annihilation process. As for example, expressions of a_0 and b_0 for $\chi\chi \rightarrow f\bar{f}$ can be expressed as,

$$a_0 = \frac{N_c n^2 \beta}{2\pi m_V^4 (m_V^2 - 4m_\chi^2)^2} [g_A^2 (g_{\chi A}^2 m_f^2 (m_V^2 - 4m_\chi^2)^2 + 2g_{\chi V}^2 m_V^4 (m_\chi^2 - m_f^2)) + g_V^2 g_{\chi V}^2 (m_f^2 + 2m_\chi^2)] \quad (11)$$

$$b_0 = \frac{3}{4} \frac{m_f^2}{m_\chi^2 - m_f^2} a_0 + \frac{N_c n^2 \beta}{48\pi m_\chi^2 m_V^4 (m_V^2 - 4m_\chi^2)^2} [12g_A^2 m_\chi^2 m_V^4 \{4m_f^2 g_{\chi V}^2 - 5m_f^2 g_{\chi A}^2 + m_\chi^2 (2g_{\chi A}^2 - g_{\chi V}^2)\} \\ + 144g_A^2 g_{\chi A}^2 m_\chi^4 m_f^2 m_V^2 + 6g_V^2 m_\chi^2 m_V^4 \{2g_{\chi A}^2 m_f^2 - 3g_{\chi V}^2 m_f^2 + m_\chi^2 (4g_{\chi A}^2 - g_{\chi V}^2)\}] \quad (12)$$

N_c is the color factor, $N_c = 1$ for leptons and 3 for quarks. $\beta = \sqrt{1 - m_f^2/m_\chi^2}$.

An approximate solution of the Boltzmann equation gives us the present mass density or relic density as the following [29],

$$\Omega_\chi h^2 = \frac{m_\chi n_\chi}{\rho_c} \simeq \frac{3 \times 10^{-27}}{\langle\sigma v\rangle} \text{cm}^3/\text{s} \quad (13)$$

where, ρ_c is the critical density of the local halo, h is the Hubble constant.

To begin with, we shall investigate the prospect of l_S being the DM candidate. We set l_S as the lightest stable particle (LSP) and N as the next to lightest particle (NLSP), the masses of other exotic fermions like E^\pm and q_S are higher than N . Consequently, the only annihilation channel available to l_S are, to a pair of SM particle via A' and Z' exchange in s-channel. l_S being an $SU(2)_{L,R}$ singlet its annihilation is controlled by the $U(1)$ gauge couplings and hyper-charges of this model. So its annihilation cross-section to SM particles is very high when the mass of l_S is almost the half of the mediator mass (A' or Z'), resulting into a reduction of relic density of l_S around its mass. The variation of relic density $\Omega_{l_S} h^2$ with its mass has been presented in Fig. 3. Equating the masses of A' and Z' to their lower limits ($m_{A'} = 3.5$ TeV, $m_{Z'} = 5.89$ TeV, see [16]) results into an annihilation cross-section finally leading to an over abundance of relic particle at present epoch. Even, near the A' and Z' resonances, annihilation cross-section is not big enough to produce the required amount of relic as measured by PLANCK. For higher values of mediating gauge boson masses, annihilation cross-section will further reduce and it would be more difficult to satisfy the relic abundance limit. In Fig. 3, we fix m_N (NLSP) at 4.1 TeV and $y_{BB} = 0$. The mass difference between N and l_S ($\Delta = |m_N - m_{l_S}|$) will play a crucial role in determining the relic. Now we discuss this issue in detail in the following.

The annihilation cross-section of NLSP (N in this case) is much higher than that of the LSP (l_S). This can be accounted by the $SU(2)$ gauge interactions of N as well as a dimension-6 four-fermi interaction (proportional to ϵ') involving N and SM quarks. So when Δ decreases (within 10 – 15% of m_{l_S}) $l_S l_S \rightarrow NN$ annihilation will increase followed by a rapid co-annihilation of $NE \rightarrow$ SM particles finally resulting into a sharp fall of relic density when m_{l_S} comes to m_N [8]. A non-zero y_{BB} may further enhance the co-annihilation $N l_S \rightarrow$ SM particles via Higgs exchange. However this also requires $\Delta \sim 0.1 - 0.15$ of m_{l_S} [8]. Thus Δ has greater control on the co-annihilation between N and l_S . We have not presented result the with non-zero y_{BB} . The above arguments explain the rapid fall of $\Omega_{l_S} h^2$ for $m_{l_S} > 3.6$ TeV in Fig. 3. So for every m_N one can obtain a particular value of the mass of l_S beyond which $\Omega_{l_S} h^2$ starts decreasing rapidly and l_S becomes under-abundant.

In the case of N being the relic particle, it is the lightest among the exotic fermions present in our model. E^\pm and N obtain masses from the same Yukawa coupling involving L_B and Φ_S , hence are degenerate in mass¹. The non-zero y_{BB} as well as electromagnetic interactions can generate a small mass splitting between E^\pm and N . A larger mass splitting between these two would allow the decay of E to N along with a W (or W_R). This in turn gives rise to non-thermal production of N which could increase the relic abundance. We have chosen the mass

¹A lower mass limit in the ballpark of a TeV, on m_{E^\pm} has been derived in [16] from the existing experimental result on long lived charged particle search at the LHC.

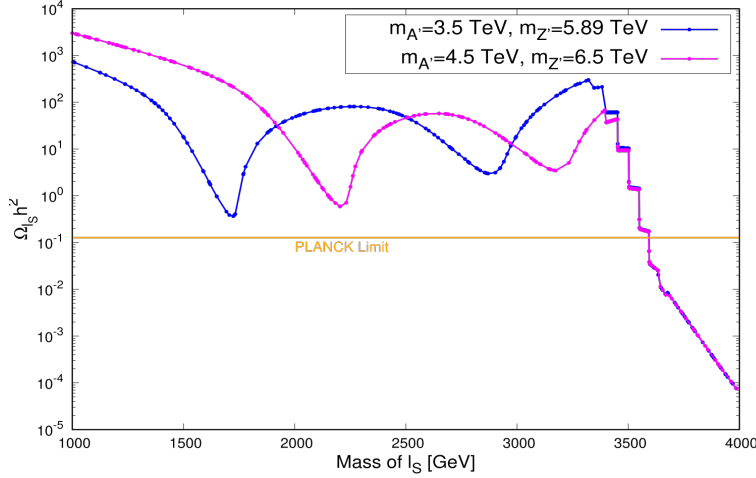


Figure 3: Mass of l_S vs relic density plot with different values of the heavy neutral gauge bosons with mass of N fixed at 4.1 TeV.

separation between E and N in such a way so that the rate of this non-thermal production is negligible compared to the thermal one [30].

Having both $SU(2)$ and $U(1)$ charges, N can couple to every SM fermions, gauge bosons and to the SM Higgs boson (via the mixing between Φ_B and Φ_S). N can thus annihilate to the SM particles with a higher rate of annihilation than that of l_S . The annihilation cross-section of N when $m_N < 270$ GeV (along with $m_{E^\pm} > 1089$ GeV), is appropriate to produce sufficient amount of relic satisfying the present experimental limits on Ωh^2 . However such a large mass splitting between N and E seems to be challenging to obtain in the model of our interest.

However, we have already pointed out that direct detection limits can only be satisfied for N , with a non-zero ϵ' and we have identified a range of values of $\frac{\epsilon'}{\Lambda'^2}$ by comparing the direct detection cross-section with experimental data. So instead of looking for low mass N , we will concentrate in the case when a non-zero value of $\frac{\epsilon'}{\Lambda'^2}$ has been assumed. Such an effective operator along with gauge interactions will contribute to the annihilation of N to a pair of SM fermions. When such allowed (by direct detection) values of $\frac{\epsilon'}{\Lambda'^2}$ have been used to estimate the annihilation cross-section of N the thermal averaged cross-section becomes too large making the relic density too small ($\sim 10^{-4}$). So N , as the relic particle, cannot simultaneously satisfy the direct detection limit and relic density limit. We also note that, with a smaller value of $\frac{\epsilon'}{\Lambda'^2}$ ($\sim 10^{-8} \text{ GeV}^{-2}$) one can satisfy the relic density constraints for a wide range of masses of N . However, such values of $\frac{\epsilon'}{\Lambda'^2}$ are in conflict with the limits obtained from the direct detection experiments. We will not present such numbers anymore.

4 Two-component Dark Matter in 32121

In the previous section we have discussed the viability of N or l_S to be the DM candidate and in the following we note down our main observations before we proceed further.

- i) N as the relic particle could satisfy the direct detection limits however having a large annihilation cross-section could not fit the bill for relic density measurement by PLANCK experiment.
- ii) On the contrary, when we choose l_S to be the relic, we are able to explain the present relic abundances data from PLANCK collaboration but direct detection cross-section is well below the limits obtained from the experiments like XENON or PICO.

Above couple of observations point to the fact that none of the above particles individually is viable to be the DM candidate or in other words none of the above can simultaneously satisfy the relic density constraint along with direct detection limits. This enforces us to consider the case of a multi-component DM scenario where N and l_S both contribute to relic density, while the direct detection limits could be fulfilled by N only.

In this section we shall investigate, in some detail, whether this two-component scenario can fulfill all the deficiencies posed by the single-component scenario discussed in previous section.

4.1 Relic Density

In a two-component dark matter scenario, let χ_1 and χ_2 are the DM particles of mass m_{χ_1} and m_{χ_2} respectively. Similarly n_1, n_2 are the corresponding number densities of the relic particles. So the Boltzmann equations are as the following [31],

$$\begin{aligned} \frac{dn_1}{dt} = & - 3Hn_1 - \langle \sigma_1 v \rangle (n_1^2 - n_1^{eq2}) - \langle \sigma_{11 \rightarrow 22} v \rangle (n_1^2 - \frac{n_1^{eq2}}{n_2^{eq2}} n_2^2) \Theta(m_{\chi_1} - m_{\chi_2}) \\ & - \langle \sigma_{22 \rightarrow 11} v \rangle (n_2^2 - \frac{n_2^{eq2}}{n_1^{eq2}} n_1^2) \Theta(m_{\chi_2} - m_{\chi_1}) - \langle \sigma v \rangle_{12} (n_1 n_2 - n_1^{eq} n_2^{eq}) \end{aligned} \quad (14)$$

$$\begin{aligned} \frac{dn_2}{dt} = & - 3Hn_2 - \langle \sigma_2 v \rangle (n_2^2 - n_2^{eq2}) - \langle \sigma_{22 \rightarrow 11} v \rangle (n_2^2 - \frac{n_2^{eq2}}{n_1^{eq2}} n_1^2) \Theta(m_{\chi_2} - m_{\chi_1}) \\ & - \langle \sigma_{11 \rightarrow 22} v \rangle (n_1^2 - \frac{n_1^{eq2}}{n_2^{eq2}} n_2^2) \Theta(m_{\chi_1} - m_{\chi_2}) - \langle \sigma v \rangle_{12} (n_1 n_2 - n_1^{eq} n_2^{eq}) \end{aligned} \quad (15)$$

where, $\langle \sigma_{1,2} v \rangle$ are the thermally averaged annihilation cross-section of a pair of χ_1 or χ_2 to lighter SM particles ($\chi_{1,2} \chi_{1,2} \rightarrow ff$), Θ is the Heaviside function. $\langle \sigma_{ii \rightarrow jj} v \rangle$ corresponds to the DM-DM conversion processes ($\chi_{1(2)} \chi_{1(2)} \rightarrow \chi_{2(1)} \chi_{2(1)}$) when kinematically allowed. The last term represents co-annihilation of two DM candidates ($\chi_1 \chi_2 \rightarrow ff$).

The total relic density Ω_χ in this scenario with N and l_S both as relic particles, can be represented as,

$$\Omega_\chi h^2 = \Omega_{l_S} h^2 + \Omega_N h^2 \quad (16)$$

In a two-component DM scenario, a gauge invariant interaction term proportional to y_{BB} present in the Yukawa Lagrangian (see Eq. 1) plays an important role. In this subsection we shall illustrate this important issue by considering both the cases with zero and non-zero y_{BB} .

To start with, let us consider $y_{BB} = 0$. So there is no mixing between N and l_S . As already discussed, the annihilation cross-section of N to SM particles is too large mainly due to the presence of a dimension-6 effective operator. Whereas the annihilation cross-section of l_S will mainly depend on the gauge couplings hence smaller than that of N . This large $\langle \sigma v \rangle$ of N will decrease the relic density of N and due to small $\langle \sigma v \rangle$ of l_S the relic abundance will be large compared to N as well as the PLANCK limit also. Such an observation has guided us to choose the mass hierarchy among N , l_S and E^\pm . We have set the mass of N lower than the mass of l_S so that annihilation of a pair of l_S to a pair of N is kinematically allowed (we shall discuss it in the end of this subsection). Such a conversion of l_S to N increases the abundance of N as well as the annihilation cross-section of l_S making the relic density of l_S a bit lower. The near mass degeneracy between E^\pm and N implies $m_{E^\pm} < m_{l_S}$. This particular choice of mass hierarchy among the exotic fermions cannot solve the whole issue completely and l_S is still over-abundant. In order to increase the annihilation cross-section of l_S significantly, we choose the mass of q_S lower than l_S but higher than the mass of N . Now, l_S can annihilate to a pair of q_S but N cannot. With this mass hierarchy, l_S and N can satisfy the PLANCK limit on the present relic density of the Universe.

But this solution has a drawback as a heavy stable colored q_S remain as relic. Probably they will form bound states with similar colored objects and contribute to relic density [32]. However, this is an issue which could be investigated independently and we will not anymore delve into this. Instead, we choose to investigate the effect of a non-zero y_{BB} which will increase the $\langle \sigma v \rangle$ of l_S even if m_{q_S} is set higher than the masses of other particles. We shall discuss our observations in the following.

A non-zero y_{BB} will open up the channels like Fig. 4. The left one (a) is the annihilation of a pair of l_S to a pair of N . The diagrams (b) and (c) represent co-annihilations between N/E and l_S where q, q' are SM particles. Here, Φ represents any one of the neutral scalars, h^0 , h_2^0 , ξ_2^0 and H_S^0 .

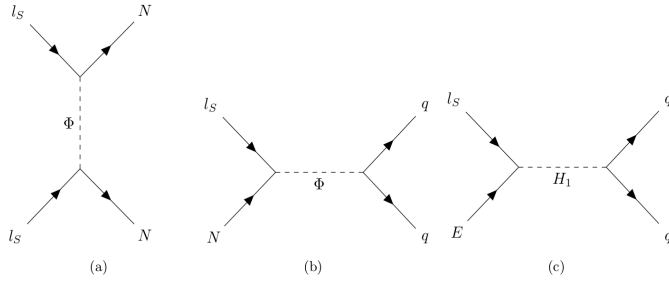


Figure 4: The DM annihilation and co-annihilation channels opened up by a non-zero y_{BB}

With a non-zero y_{BB} , the diagram (b) in Fig. 4 leads to a higher annihilation rate for l_S and N , reducing their relic abundances. However, this annihilation rate also crucially depends on the mass difference between N and l_S ($\Delta = |m_{l_S} - m_N|$). As Δ decreases the cross-section of the co-annihilation increases reducing the relic abundance of l_S . So, clearly there is a correlation between Δ and y_{BB} which is shown in Fig. 5. Diagram (c) is only important in case of third-generation of quarks (t, b) as the couplings of H_1^\pm to the other SM quarks and leptons are negligibly small [16]. Moreover, E^\pm is heavier than N in mass. Consequently, the mass difference between l_S and E is larger than that of l_S and N . So while discussing about the co-annihilation of l_S , the contribution of diagram (b) will be larger than that from diagram (c).

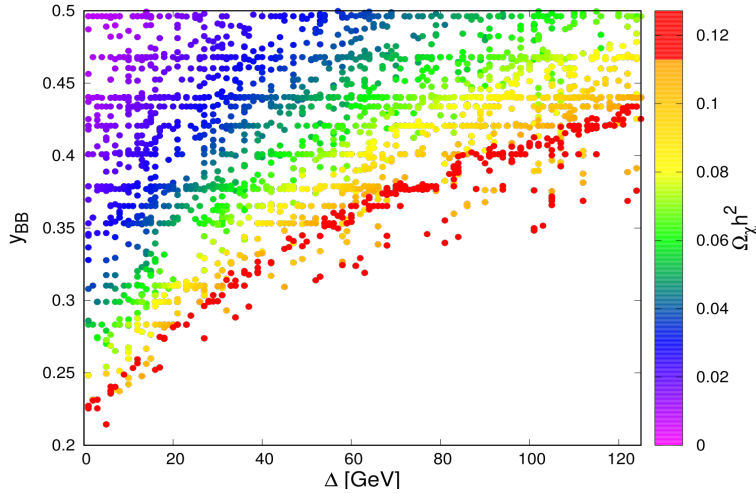


Figure 5: The correlation between y_{BB} and the mass difference between N and l_S has been presented. The red blobs show the allowed points satisfying the PLANCK limit on relic density within 2σ band.

In Fig. 5, the above correlation between Δ and y_{BB} is evident. A large Δ decreases the annihilation cross-section which can be enhanced by asking for a larger y_{BB} . For a non-zero y_{BB} , l_S can decay to N and a SM-like Higgs h^0 ($l_S \rightarrow N h^0$, onshell or offshell). In order to reduce this decay rate, we choose $\delta < 125$ GeV. It is important to note that a higher value of y_{BB} also decreases the relic abundance of N via the co-annihilation with l_S (Fig. 4 (b)). The red points represent the allowed values of Ω_χ within 2σ error band given by PLANCK collaboration.

For the present analysis with N and L_S as dark matter particles we have fixed the value of ϵ'/Λ'^2 (8.16×10^{-6} GeV $^{-2}$). We have already mentioned that the annihilation of N is sensitive to this parameter. This particular choice of ϵ'/Λ'^2 (8.16×10^{-6} GeV $^{-2}$) is chosen such that for any value of m_N the direct detection limit could be satisfied which is evident from Fig. 2. In Fig. 6, we present the relative abundance of l_S (i.e., Ω_{l_S}/Ω_χ) with the mass of l_S for different values of y_{BB} . Over a wide range of mass of l_S , it contributes dominantly to relic density. This is mainly due to its lower interaction rate compared to N . From Fig. 6 (for $\epsilon'/\Lambda'^2 = 8.16 \times 10^{-6}$ GeV $^{-2}$), one can see that N can at most contribute 10-12% to Ω_χ . In this context, it needs to be mentioned that, the value of the relative abundance of N , Ω_N/Ω_χ increases with decreasing ϵ'/Λ'^2 (as a lower value of ϵ'/Λ'^2 will decrease

the annihilation rate of N). With a higher mass of N , the allowed range of ϵ'/Λ'^2 becomes broader i.e., a lower value of this effective coupling becomes allowed (see Fig. 2). Thus we can obtain a higher relative abundance of N for a heavier N .

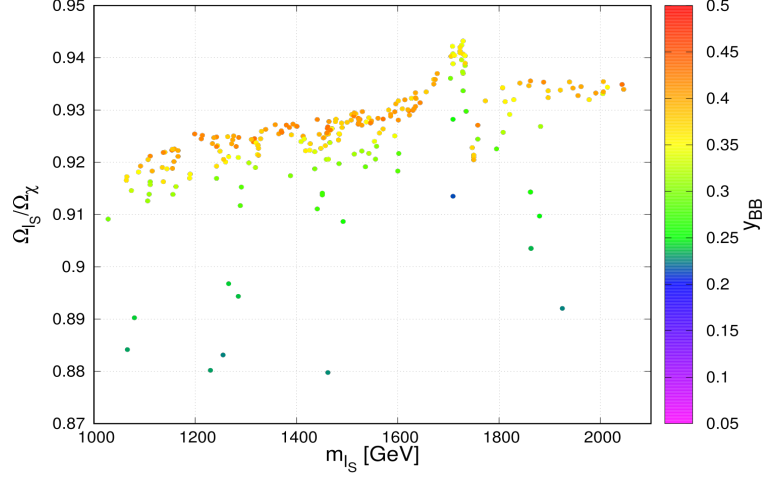


Figure 6: Variation of the relative abundance of l_S (Ω_{l_S}/Ω_χ) with respect to mass of l_S and y_{BB} . Relative abundance of N can be understood as $1 - \Omega_{l_S}/\Omega_\chi$.

In the early Universe, the conversion of one relic particle to the other can significantly change the relic abundances of each particle. In general, the pair of heavier DM particle can convert to a pair of lighter DM candidate which can increase the abundance of the lighter one.

To illustrate this issue in our case with $m_{l_S} > m_N$, we have presented relic density for N in a single-component DM scenario and a two-component DM scenario in Fig. 7. One can see, even with $y_{BB} = 0$ the contribution of N to relic density increases significantly in a two-component scenario mainly due to the conversion of $l_S l_S \rightarrow NN$. While making this plot we have set $m_{l_S} = 3$ TeV.

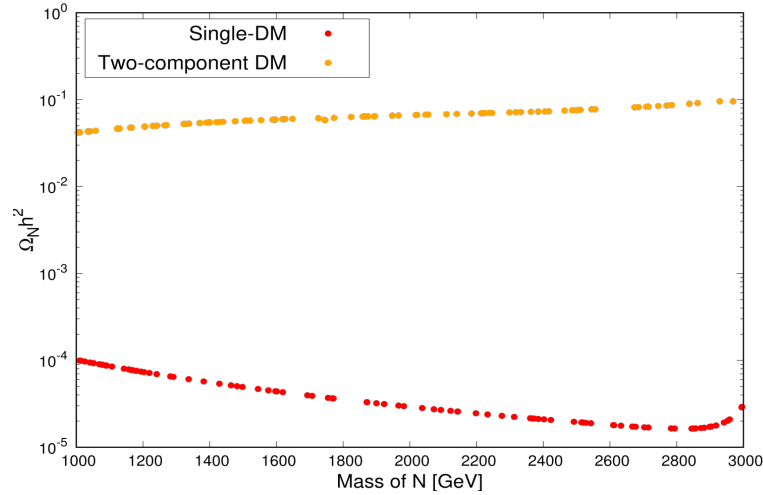


Figure 7: The variation of relic density of N between a two-component DM scenario (orange dots) and single DM scenario (red dots) due to $l_S l_S \rightarrow NN$ conversion for $y_{BB} = 0$. Here m_{l_S} has been set to 3 TeV.

4.2 Direct Detection

In case of a two-component dark matter model, the expression for the direct detection cross-section can be expressed as,

$$\sigma = \left(\frac{\Omega_N}{\Omega_\chi} \right) \sigma_N + \left(\frac{\Omega_{l_S}}{\Omega_\chi} \right) \sigma_{l_S} \quad (17)$$

Individual cross-section of N and l_S , σ_N and σ_{l_S} , the spin-independent and dependent cross-section has already been discussed in section 3. So with the knowledge of relative abundances of N and l_S one can easily calculate the direct detection cross-section. As for example, in Fig. 8, we have presented the spin-dependent scattering cross-section of N (as the contribution of l_S to σ will be negligible compared to N even after having a larger relative abundance) as a function of ϵ'/Λ'^2 for two different values of y_{BB} . We also compare this cross-section with experimental upper limit from XENON. So in this two-component scenario a new limit on ϵ'/Λ'^2 ($6.6 - 10.28 \times 10^{-6} \text{ GeV}^{-2}$ for $y_{BB} = 0.3$ and $6.5 - 10.37 \times 10^{-6} \text{ GeV}^{-2}$ for $y_{BB} = 0.41$) has been obtained from this analysis. The limits have a little sensitivity on the choice of values of y_{BB} as this parameter controls the co-annihilation of N with l_S . It is evident from the plot that the allowed range of ϵ'/Λ'^2 is wider than in the case of the single-component DM (N). This can be explained by the reduced relative abundance of N in case of a two-component DM.

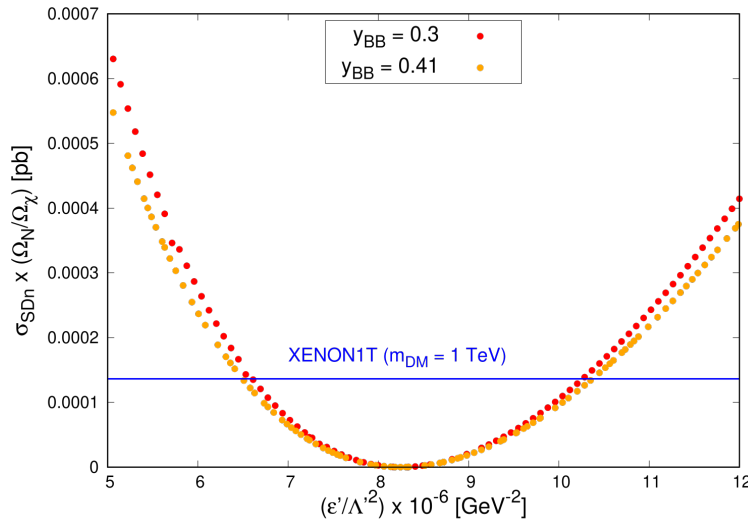


Figure 8: Variation of spin-dependent scattering cross-section for a 1 TeV N mass with the coefficient ϵ'/Λ'^2 . The red and orange solid points represent the cases for $y_{BB} = 0.3$ and 0.41 respectively.

5 Conclusion

To summarise, we have investigated phenomenological implications of a LR symmetric model based on E_6 inspired gauge group $SU(3)_C \otimes SU(2)_L \otimes U(1)_L \otimes SU(2)_R \otimes U(1)_R$ from the perspective of Dark Matter. There are two charge neutral fermions among the **27**-plet of fermions of E_6 that we have considered in our analysis. We have investigated in some details the prospect of these two heavy fermions to be a candidate for relic particle. One of these, N , is charged under both $SU(2)$ s and $U(1)$ s transformations. The other one l_S carries $U(1)$ charges however singlet under both the $SU(2)$ s.

To begin with, we have considered the scenario, in which any one of these neutral fermions acts as the relic particle. N has a large annihilation rate along with large direct detection cross-section at an experiment like XENON. To bring the direct detection cross-section of N below the experimental limits, we consider a dimension-6 4-fermion effective interaction involving a pair of N s and a pair of SM fermions. By appropriately adjusting the coefficient of this operator one can easily make the direct-detection rate of N consistent with the experimental data, however, this will also change the annihilation rate of N in such a way that relic density constraint could not be satisfied.

We then turn our attention to l_S . l_S being an $SU(2)$ singlet, has appropriate annihilation rates for producing the amount of relic which satisfies the experimental data for some chosen masses of l_S and N which is now the NLSP. However, the smaller interaction rate of l_S , prohibits itself from satisfying the direct detection limits.

The above observations, force us to abandon the idea of a single DM candidate in the model we are interested in. Consequently, we turn to the case of a two-component DM scenario where both the N and l_S contributes to relic density. However, only N takes part in the direct detection process.

N and l_S both being relic particles, their relative mass hierarchy plays a crucial role in the analysis. If N is heavier, then annihilation of N to l_S increases producing a large density of l_S but l_S having lower annihilation rate, would not annihilate sufficiently thus producing a situation with more than necessary relic density at present time.

The other alternative, is to keep l_S heavier than N . In such a scenario, l_S can produce N via annihilation followed by annihilation of N to SM particles via gauge interaction and via the effective 4-fermion interaction. However, the relative mass hierarchy among N and l_S and other exotic particles like q_S and E also plays a crucial role in determining the relic density. Making, l_S heavier than q_S (and E), would force l_S to annihilate more to q_S and E pairs and will yield a relic density which is in agreement with the experiments. Both q_S and E probably result into SM particles via gauge interactions. However due to the expansion of the Universe, the rate of such annihilations of q_S and N will be reduced and probably result into some remnant q_S or E at present epoch along with N and l_S . To avoid such a circumstance, we keep the masses of q_S heavier than l_S and N . E having gauge interactions, will probably decay to N along with a SM particle (possibly a W) and would contribute to the relic of N .

Making q_S and N heavier than l_S would reduce the annihilation of l_S to such an extent that it would produce more relic than necessary at the present time. To overcome such a situation, a trilinear interaction involving N , l_S and the SM Higgs boson will play a very crucial role. Presence of such an interaction with appropriate mass difference between N and l_S will control the co-annihilation between these particles thus restores the annihilation rate of these particles to yield the right amount of relic density.

We now turn our attention to the direct detection cross-sections involving N and l_S . The effective direct detection cross-section is a combination of the direct detection rates of the individual species weighted by their relative abundances (relic density fractions). Although l_S has a higher relative abundance, its contribution will be negligible compared to its partner N due to its negligibly small direct detection cross-section. It is worth to mention that the direct detection cross-section of N is sensitive to ϵ'/Λ'^2 , the coefficient of dimension-6 operator, leading to its annihilation to a pair of SM fermions. For a given mass of N , we found a range of values of ϵ'/Λ'^2 allowed by the direct detection experiment like XENON.

We have observed that in all possible scenarios that we have considered, rates of indirect detection (DM annihilation to pair of SM particles) of N and l_S is far below than the experimental data from Fermi-LAT. Consequently, one cannot put a meaningful constraint on the model parameters from such an experiment.

Before we finally conclude it is interesting to note that pair production cross-section of l_S at 27 (14) TeV LHC will be nearly 3 (0.2) fb for l_S mass of 1 TeV. Once produced, l_S will decay to a SM Higgs boson and an N , resulting into di-Higgs plus missing p_T signature. Assuming the Higgs tagging efficiency to be 50% [33], 3 (0.2) fb cross-section will yield nearly 2000 (150) di-Higgs events with 3 ab^{-1} luminosity. This particular signal is almost free of SM background. However, this method crucially depend on the Higgs tagging which has been a fairly well developed technique at the LHC [33].

Acknowledgement : S. B. acknowledges financial support from DST, Ministry of Science and Technology, Government of India in the form of an INSPIRE-Senior Research Fellowship.

References

- [1] PLANCK collaboration, N. Aghanim *et al.*, *Planck 2018 results VI. Cosmological parameters*, *Astronomy & Astrophysics* **641**, A6 (2020), arXiv: [1807.06209].
- [2] C. L. Bennett *et. al.*, *Nine-Year Wilkinson Microwave Anisotropy Probe (WMAP) Observations: Final Maps and Results*, *Astrophys.J.* **208** (Oct., 2013) 20, arXiv: [1212.5225].
- [3] AMS collaboration, S.-J. Lin, X.-J. Bi, P.-F. Yin and Z.-H. Yu, *Implications for dark matter annihilation from the AMS-02 \bar{p}/p ratio*, arXiv: [1504.07230].

- [4] PAMELA collaboration, O. Adriani *et al.*, *Measurement of the flux of primary cosmic ray antiprotons with energies of 60-MeV to 350-GeV in the PAMELA experiment*, [ETP Lett. 96 \(2013\) 621–627](#).
- [5] Fermi-LAT collaboration, M. Ackermann *et al.*, *Searching for Dark Matter Annihilation from Milky Way Dwarf Spheroidal Galaxies with Six Years of Fermi Large Area Telescope Data*, [Phys. Rev. Lett. 115, 231301 \(2015\)](#), arXiv: [1503.02641].
- [6] Fermi-LAT and MAGIC collaboration, M. L. Ahnen *et al.*, *Limits to dark matter annihilation cross-section from a combined analysis of MAGIC and Fermi-LAT observations of dwarf satellite galaxies*, [JCAP 02 \(2016\) 039](#), arXiv: [1601.06590].
- [7] ATLAS collaboration, G. Aad *et al.*, *Observation of a new particle in the search for the Standard Model Higgs boson with the ATLAS detector at the LHC*, [Phys. Lett. B 716 \(2012\) 1–29](#), arXiv: [1207.7214]; CMS collaboration, S. Chatrchyan *et al.*, *Observation of a New Boson at a Mass of 125 GeV with the CMS Experiment at the LHC*, [Phys. Lett. B 716 \(2012\) 30](#), arXiv: [1207.7235].
- [8] G. Jungman, M. Kamionkowski and K. Griest, *Supersymmetric Dark Matter*, [Physics Reports 267 \(1996\) 195–373](#), arXiv: [hep-ph/9506380].
- [9] C. Muñoz, *Models of Supersymmetry for Dark Matter*, [EPJC Conf, 2017](#), arXiv: [1701.05259].
- [10] D. Hooper and S. Profumo, *Dark Matter and Collider Phenomenology of Universal Extra Dimensions*, [Phys.Rept.453:29–115,2007](#), arXiv: [hep-ph/0701197].
- [11] ATLAS and CMS Collaborations, C. Autermann, *Search for supersymmetry at the LHC*, [EPJ Web Conf. 164 \(2017\) 01028](#); A. Canepa, *Searches for supersymmetry at the Large Hadron Collider*, [Reviews in Physics 4 \(2019\) 100033](#); CMS Collaboration, *Search for resonant and nonresonant new phenomena in high-mass dilepton final states at $\sqrt{s} = 13$ TeV*, [JHEP07 \(2021\) 208](#), arXiv: [2103.02708]; CMS Collaboration, *Search for Large Extra Dimensions in the Diphoton Final State at the Large Hadron Collider*, [JHEP05 \(2011\) 085](#), arXiv: [1103.4279]; CMS Collaboration, *Search for new physics with dijet angular distributions in proton-proton collisions at $\sqrt{s} = 13$ TeV*, [JHEP 07 \(2017\) 013](#), arXiv: [1703.09986].
- [12] A. Freitas, P. Schwaller and D. Wyler, *A Little Higgs Model with Exact Dark Matter Parity*, [JHEP 0912:027,2009](#), arXiv: [0906.1816].
- [13] R. Campbell, S. Godfrey, H. E. Logan and A. Poulin, *Real singlet scalar dark matter extension of the Georgi-Machacek model*, [Phys. Rev. D 95, 016005 \(2017\)](#), arXiv: [1610.08097].
- [14] D. Nanda and D. Borah, *Common origin of neutrino mass and dark matter from anomaly cancellation requirements of a U_{B-L} model*, [Phys. Rev. D 96, 115014](#).
- [15] Q. Shafi, *E_6 as a unifying gauge symmetry*, [Physics Letters B, 79\(3\), 301–303](#); F. Gürsey, P. Ramond and P. Sikivie, *A universal gauge theory model based on E_6* , [Physics Letters B, 60\(2\), 177–180](#).
- [16] S. Bhattacharyya and A. Datta, *Phenomenology of an E_6 inspired extension of Standard Model: Higgs sector*, [Phys. Rev. D 105, 075021](#), arXiv: [2109.08524].
- [17] B. Barman, S. Bhattacharya, P. Ghosh, S. Kadam and N. Sahu, *Fermion dark matter with scalar triplet at direct and collider searches*, [Phys. Rev. D 100, 015027](#), arXiv: [1902.01217]; C. Bonilla, L. M. G. de la Vega, J. M. Lamprea, R. A. Lineros and E. Peinado, *Fermion Dark Matter and Radiative Neutrino Masses from Spontaneous Lepton Number Breaking*, [New Journal of Physics, Vol. 22, March 2020](#), arXiv: [1908.04276]; S. Choubey, S. Khan, M. Mitra and S. Mondal, *Singlet-triplet fermionic dark matter and LHC phenomenology*, [Eur. Phys. J. C 78, 302 \(2018\)](#), arXiv: [1711.08888]; A. Carmona, J. C. Ruiz and M. Neubert, *A warped scalar portal to fermionic dark matter*, [Eur. Phys. J. C 81, 58 \(2021\)](#), arXiv: [2011.09492]; E. Bernreuther, S. Heeba and F. Kahlhoefer, *Resonant Sub-GeV Dirac Dark Matter*, [JCAP 2021 \(2021\) no. 03, 040](#), arXiv: [2010.14522]; B. Chauhan, *Sub-MeV Self Interacting Dark Matter*, [Phys. Rev. D 97, 123017 \(2018\)](#), arXiv: [1711.02970].

- [18] C. D. R. Carvajal, R. Longas, O. Rodríguez and Ó. Zapata, *Singlet fermion dark matter and Dirac neutrinos from Peccei-Quinn symmetry*, *Phys. Rev. D.* **105**, 015003, arXiv: [2110.15167].
- [19] T. Bandyopadhyay and R. Maji, *The E_6 route to multicomponent dark matter*, arXiv: [1911.13298].
- [20] ATLAS collaboration, M. Aaboud *et al.*, *Combination of searches for invisible Higgs boson decays with the ATLAS experiment*, *Phys. Rev. Lett.* **122**, 231801 (2019), arXiv: [1904.05105]; CMS collaboration, A. M. Sirunyan *et al.*, *Search for invisible decays of a Higgs boson produced through vector boson fusion in proton-proton collisions at $\sqrt{s} = 13$ TeV*, *Phys. Lett. B* **793** (2019) 520, arXiv: [1809.05937].
- [21] R. Barbieri, L. J. Hall and V. S. Rychkov, *Improved Naturalness with a Heavy Higgs: An Alternative Road to LHC Physics*, *Phys. Rev. D* **74**:015007 (2006), arXiv: [hep-ph/0603188].
- [22] XENON collaboration, E. Aprile *et al.*, *Dark Matter Search Results from a One Tonne \times Year Exposure of XENON1T*, *Phys. Rev. Lett.* **121**, 111302 (2018), arXiv: [1805.12562]; XENON collaboration, E. Aprile *et al.*, *Constraining the Spin-Dependent WIMP-Nucleon Cross Sections with XENON1T*, *Phys. Rev. Lett.* **122**, 141301 (2019), arXiv: [1902.03234].
- [23] LUX Collaboration, D. S. Akerib *et al.*, *Limits on Spin-Dependent WIMP-Nucleon Cross Section Obtained from the Complete LUX Exposure*, *PRL* **118**, 251302 (2017), arXiv: [1705.03380].
- [24] PICO Collaboration, C. Amole *et al.*, *Dark Matter Search Results from the PICO-60 C_3F_8 Bubble Chamber*, *Phys. Rev. Lett.* **118**, 251301 (2017), arXiv: [1707.07666].
- [25] PANDA-II Collaboration, J. Xia *et al.*, *PandaX-II Constraints on Spin-Dependent WIMP-Nucleon Effective Interactions*, *Physics Letters B* **792C** (2019) 193-198, arXiv: [1807.01936].
- [26] A. Berlin, D. Hooper and S. D. McDermott, *Simplified Dark Matter Models for the Galactic Center Gamma-Ray Excess*, *Phys. Rev. D* **89**, 115022 (2014), arXiv: [1404.0022].
- [27] A. Alloul, N. D. Christensen, C. Degrande, C. Duhr and B. Fuks, *FeynRules 2.0 - A complete toolbox for tree-level phenomenology*, *Comput.Phys.Commun.* **185** (2014) 2250-2300, arXiv: [1310.1921].
- [28] G. Bélanger, A. Mjallal and A. Pukhov, *Recasting direct detection limits within micrOMEGAs and implication for non-standard Dark Matter scenarios*, *Eur. Phys. J. C* **81**no. 3, (2021) 239, arXiv: [2003.08621].
- [29] M. Srednicki, R. Watkins and K. A. Olive, *Calculations of Relic Densities in the Early Universe*, *Nuclear Physics B* **310** (1988) 693-713.
- [30] P. S. Dev, A. Majumdar and S. Qutub, *Constraining non-thermal and thermal properties of Dark Matter*, *Front. Phys.*, 09 May 2014, arXiv: [1311.5297].
- [31] A. Ahmed, M. Duch, B. Grzadkowski and M. Iglicki, *Multi-component dark matter: the vector and fermion case*, *Eur. Phys. J. C* (2018) 78:905, arXiv: [1710.01853]; A. Betancur, G. Palacio and A. Rivera, *Inert doublet as multicomponent dark matter*, *Nucl. Phys. B*, 2020, 115276, arXiv: [2002.02036]; J. Edsjo and P. Gondolo, *Neutralino Relic Density including Coannihilations*, *Phys. Rev. D* **56**:1879-1894,1997, arXiv: [hep-ph/9704361].
- [32] V. De Luca, A. Mitridate, M. Redi, J. Smirnov and A. Strumia, *Colored Dark Matter*, *Phys. Rev. D* **97**, 115024 (2018), arXiv: [1801.01135].
- [33] B. Bhattacharjee, A. Chakraborty, D. K. Ghosh and S. Raychaudhuri, *Using Jet Substructure at the LHC to Search for the Light Higgs Bosons of the CP-Violating MSSM*, *Phys. Rev. D* **86**, 075012 (2012), arXiv: [1204.3369].